ANTIOXIDANTS & REDOX SIGNALING
Volume 14, Number 11, 2011

DOI: 10.1089/ars.2010.3491

Retinoic Acid Induces Autophagosome Maturation Through Redistribution of the Cation-Independent Mannose-6-Phosphate Receptor

Yogendra Rajawat, Zoe Hilioti, and Ioannis Bossis

Abstract

Retinoic acids (RAs) have diverse biologic effects and regulate several cellular functions. Here, we investigated the role of RA on autophagy by studying its effects on autophagosome (AUT) maturation, as well as on upstream regulators of autophagosome biogenesis. Our studies, based on the use of pH-sensitive fluorescent reporter markers, suggested that RA promotes AUT acidification and maturation. By using competitive inhibitors and specific agonists, we demonstrated that this effect is not mediated by the classic RAR and RXR receptors. RA did not affect the levels of upstream regulators of autophagy, such as Beclin-1, phospho-mTOR, and phospho-Akt1, but induced redistribution of both endogenous cation-independent mannose-6-phosphate receptor CIMPR and transiently transfected GFP and RFP full-length CIMPR fusion proteins from the trans-Golgi region to acidified AUT structures. Those structures were found to be amphisomes (acidified AUTs) and not autophagolysosomes. The critical role of CIMPR in AUT maturation was further demonstrated by siRNA-mediated silencing of endogenous CIMPR. Transient CIMPR knockdown resulted in remarkable accumulation of nonacidified AUTs, a process that could not be reversed with RA. Our results suggest that RA induces AUT acidification and maturation, a process critical in the cellular autophagic mechanism. *Antioxid. Redox Signal.* 14, 2165–2177.

Introduction

Autophagy is a ubiquitous intracellular catabolic process that involves the bulk degradation of cytoplasmic components through a lysosomal pathway. This process is characterized by the engulfment of part of the cytoplasm inside double-membrane vesicles called autophagosomes (AUTs). AUTs subsequently fuse with lysosomes to form an autophagolysosome in which the cytoplasmic cargo is degraded and the degradation products are recycled for the synthesis of new molecules (41). The autophagic machinery actually mediates the majority of intracellular housekeeping tasks, such as the turnover of most long-lived proteins, macromolecules, biologic membranes, and whole organelles, including mitochondria, ribosomes, endoplasmic reticulum, and peroxisomes (6).

Nutrient availability is one of the best-characterized factors involved in regulation of autophagy. The great sensitivity of the autophagic response to the nutritional state implies that certain macro- or micronutrients regulate this response. In general, macronutrient (proteins, carbohydrates, lipids) availability suppresses autophagy. Macronutrient deprivation, and especially reduction in certain intracellular glucogenic amino acids, mainly glutamine, triggers the autophagic protein degradation (44), whereas the presence of some amino acids (leucine, tyrosine, and phenylalanine) is sufficient to inhibit autophagy in various cell types (20, 32). Carbohydrates have not been shown to affect autophagy directly; however, they may act indirectly through their effects on insulin and insulin receptor (22). Carbohydrates are mostly broken down and become available to cells as glucose. An increase in systemic glucose concentration induces insulin secretion, which causes activation of mTOR and suppression of autophagy. An increase in cellular glucose uptake results in enhanced levels of ATP production, which in turn lead to constitutive activation of the insulin receptor and suppression of autophagy. Lipids can affect autophagy indirectly through the insulin/glucagon signaling pathway (12, 16) and cholesterol metabolism (5), or directly, as increased intracellular lipid content was recently shown to impair autophagy (46).

With the exception of certain vitamins, the effect of various dietary micronutrients on autophagy has not been examined. Most vitamins studied have been found to stimulate autophagy. Treatments of pancreatic stellate cells with tocotrienols (vitamin E compounds), H1299 non–small lung carcinoma cells with vitamin C, HL-60 leukemia cells with vitamin K_2,

Department of Veterinary Medicine, University of Maryland, College Park, Maryland.

and MCF-7 breast cancer cells with vitamin D_3 induced an increase in AUTs and other acidic vesicular structures (15, 36, 42, 49). The mechanism by which vitamins C, E, and K_2 increased autophagic activity in the previous studies has not been delineated. Induction of autophagy by vitamin D_3 and analogues was found to be mediated by an increase in intracellular calcium levels, which in turn affect the mTOR signaling cascade.

Retinoic acid (RA) has diverse biologic effects in the control of cell growth and differentiation and regulates the expression of specific networks of genes through two families of nuclear receptors, the RA receptors (RARs) and the retinoid X receptors (RXRs) (10). These receptors belong to the steroid-thyroid hormone receptor superfamily, which regulates gene transcription through binding to specific DNA sequences, resulting in an increased or decreased synthesis of specific proteins (47). In addition to the effects of retinoic acid through RARs and RXRs, evidence (1, 8, 35) suggests that other retinoid response pathways that are independent of the nuclear receptors may exist. Despite our knowledge of the diverse effects of retinoic acid on several cellular functions, its effect on autophagy has not been studied. Interestingly, photoaffinity-labeling studies have shown direct binding of RA to the cation-independent mannose-6-phosphate/IGFII receptor (CIMPR) with high affinity (21).

CIMPR is a 300-kDa (2,491 amino acids) multiple ligand-binding cell transmembrane glycoprotein, ubiquitously expressed in human tissues. This receptor has been shown to play a fundamental role in a variety of physiologic processes such as lysosomal enzyme trafficking, endocytosis and lysosomal degradation of extracellular ligands, and regulation of apoptotic and mitogenic effects (14). The first 40 amino acids (aa) in CIMPR represent a cleavable signal peptide. The major part of the protein, 2,264 aa, consists of a large extracellular domain (or luminal in the Golgi and endosomal compartments), a very short 23-aa transmembrane domain, and a 164-aa cytoplasmic domain constituting the C-terminus (33). The extracellular domain is composed of 15 homologous repeats, 134 to 167 aa long, which represent 15 structural units (37). This structural arrangement in the extracellular globular domain indicates multifunctional binding properties. CIMPR is localized primarily in intracellular compartments, the trans-Golgi network (TGN), and acidic endosomal and prelysosomal compartments, the exact nature of which has not been fully characterized, and only 5% to 10% is present on the cell surface (25). The primary function of CIMPR is to sort and transport mannose-6-phosphate (M6P)-bearing glycoproteins from TGN to endosome/lysosomes (25). In addition, CIMPR can bind extracellular ligands, mediate endocytosis of IGF-2, and urokinase-type plasminogen activator receptor (9); participate in the activation of latent transforming growth factor β (34); and bind RA. The binding site for RA is not known; however, it is distinct from those for M6P and IGF2 on the receptor (21).

From the present study, we present evidence indicating that ATRA induces acidification of AUTs (amphisomes) through a mechanism independent of the classic retinoid receptors. We found that ATRA induces redistribution of CIMPR from the perinuclear TGN region to vesicular structures that include acidified AUTs. siRNA-mediated knockdown of CIMPR resulted in remarkable accumulation of CFP-LC3–labeled nonacidified autophagosomes, a process that could not be reversed with ATRA treatment. Moreover, CIMPR knockdown resulted in accumulation of Rab9-positive endosomes, and reduced acidification of lysosomes but not their abundance. Our results suggest that ATRA induces AUT acidification and maturation either by direct redistribution of the CIMPR to AUTs or by increasing fusion of immature AUTs with acidified late endosomes.

Materials and Methods

Reagents and Antibodies

All *trans*-retinoic acid (ATRA) was obtained from Sigma (no. R2625). CD2665, a selective RAR$\beta/\gamma/\alpha$ antagonist (no. 3800) and docosahexaenoic acid (DCHA), a selective retinoid X receptor (RXR) agonist (no. 3687) were purchased from Tocris Biosciences, Bristol, UK. Rapamycin (no. 553210) was procured from Calbiochem (La Jolla, CA). Retinoids were dissolved in DMSO at a concentration of 10 m*M* and were stored under N2 in the dark at -80°C. Stock solutions were diluted to the appropriate concentrations with growth medium just before use. The antibody against light chain 3 protein (LC3) (nno. M115-3; clone no. 51-11) was from MBL International Corp.; the monoclonal antibodies against CIMPR for use in immunofluorescence staining were from Abcam (no. 2733-100, clone 2G-11), and for Western blotting, from Biolegend (no. 315902, clone-MEM238); the rabbit polyclonal antibody against Atg6/Beclin-1 (BECN1) was from Abgent (no. AP-1818b). The rabbit anti-mTOR polyclonal antibody was from Sigma (no. T2959). The rabbit monoclonal anti-phospho-mTOR (no. 2971), rabbit monoclonal antibody against Akt (pan) (no. 4691; clone-C67E7), and anti-phospho-Akt1 (no. 4058; clone-193H12) were from Cell Signaling Technologies. Anti-GFP rabbit polyclonal antibody (no. sc-8334), anti-actin mouse monoclonal antibody (no. sc-8432), goat anti-mouse-IgG-HRP (no. sc-8432), and bovine anti-rabbit-IgG-HRP (no. sc-2370) were from Santa Cruz Biotechnology. For immunocytochemistry, Alexa Fluor-555 goat anti-mouse IgG (no. A21422) secondary antibody was from Molecular Probes, Eugene, Oregon. LysoSensor Green DND-189 (no. L-7535), a pH indicator probe, was from Molecular Probes.

Cell line and plasmid constructs

HeLa cells were cultured in Dulbecco's modified Eagle's medium (DMEM) supplemented with 10% heat-inactivated fetal bovine serum, 1% nonessential amino acids, 10 m*M* sodium pyruvate, 2 m*M* glutamine, 50 IU/ml penicillin, and 50 μg/ml streptomycin, in a humidified 95% air/5% CO_2 atmosphere at 37°C. For generation of the CFP-LC3 stable cell line, HeLa cells were transfected by a plasmid encoding CFP-LC3. The transfected cells were initially selected with G418 (Sigma; no. G8168) at 500 μg/ml of culture media for 2 weeks. Fluorescent cells were subsequently sorted with FACS, and individual clones were isolated by the limited-dilution method. Stable clones were maintained in medium supplemented with 300 μg/ml of G418.

In all experiments ATRA was used at 1 μM. All transfections were performed by using TransPass HeLa transfection reagent (no. M2556S) from New England Biolabs (NEB). Plasmid encoding CFP-LC3 used in this study was described previously (28). mCherry-LC3 was prepared by digesting pCFP-LC3 with *Eco*R1/*Bam*H1 and subcloning of the LC3

ORF into the *Eco*R1/*Bam*H1 sites of pmCherry-C1 (Clontech). The pmCherry-GFP-LC3 construct was a generous gift from Dr. Terje Johansen. Lamp1-mRFP plasmid construct was obtained from Addgene (Addgene plasmid 1817). pCerulean-Rab5, pCerulean-Rab7, and pCerulean-Rab9 constructs used in this study were described previously (28). For generating CIMPR mGFP and mRFP fusion constructs, cellular mRNA was isolated from HeLa cells by using the Trizol method. CIMPR cDNA was prepared by using Protoscript-II RT-PCR kit (no. E6400S) from NEB. Amino acids 110-2491 from the CIMPR ORF were directly amplified from the cDNA by using a forward primer (ctggaattcaacacaacagtg) containing the only *Eco*RI site in the sequence and a reverse primer (ctgaccgg taaGATgtgtaagaggtcctcgtc) containing a unique *Age*I site. The three capital letters indicate in reverse orientation the last amino acid of the CIMPR ORF. The PCR product was digested with *Eco*RI/*Age*I and cloned in frame at the *Eco*RI/*Age*I sites of plasmid mGFP-N1. The ORF encoding the first 109 amino acids and also a Kozac sequence and *Xho*I/*Eco*RI flanking sites were artificially synthesized (Genescript Inc.) and subcloned in the *Xho*/*Eco*RI sites of the mGFP-N1 vector containing amino acids 110-2491, thus creating CIMPR-mGFP. An *Xho*/*Age*I site from the last vector was also subcloned in the *Xho*I/*Age*I sites of plasmid mRFP-N1 to create CIMPR-mRFP. These constructs therefore express the full ORF of CIMPR, including the signal peptide, and the fluorescent tag is placed in the c-terminus of CIMPR. The c-terminus of CIMPR is exposed toward the cytosol, and fluorescent tags such as GFP are not subject to pH-mediated quenching in acidified organelles.

RNA interference studies

HeLa cells were transfected with annealed double-stranded Silencer select validated siRNA against CIMPR from applied biosystem (siRNA ID no. s7217) as designated in the experiments by using the manufacturer's suggested protocol. The sequence for the siRNA used is CUACCUGUAUGAG AUCCAAtt (sense) and UUGGAUCUCAUACAGGUAGtt (antisense). Chemical treatments in transfected cells were initiated 8 h after transfection, and cells were analyzed 48 h after transfection.

General methods

To obtain total cell lysates after a designated incubation period with various treatments, cells were washed twice with ice-cold PBS, lysed in RIPA buffer [150 m*M* NaCl, 50 m*M* Tris-HCl (pH 8.0), 0.1% Nonidet P-40, 0.5% deoxycholate, 0.1% sodium dodecylsulfate (SDS), protease inhibitor cocktail (Sigma), and phosphatase inhibitor cocktail], and clarified by high-speed centrifugation. For Western blot analysis, equal amounts of total protein were separated by SDS-PAGE and then transferred to nitrocellulose membranes. Membranes were blocked with blocking buffer (TBST-1% casein) for 1 h, probed with primary antibodies for 2 h and then incubated with the HRP-conjugated secondary antibody for 1 h. Antibody binding was detected by enhanced chemiluminescence (Amersham). Density for each band was analyzed by using a densitometer. Equal protein loading was confirmed by probing against β-actin. Values obtained for phosphorylated mTOR and phosphorylated Akt1 were normalized to total mTOR and total Akt density, respectively. For immunofluorescence, cells were grown on chambered coverslips. At the end of the experimental treatment, the cells were fixed with 4% paraformaldehyde in 0.1 *M* phosphate buffer (15 min), washed with wash buffer (PBS/0.1% saponin), blocked for 1 h with blocking buffer (PBS/1% BSA/0.1% saponin), and sequentially incubated with the primary and secondary antibodies in blocking buffer. After the final wash, the chambers were filled with mounting media (80% glycerol, 100 m*M* Tris, pH 8) containing antifade (DABCO) and analyzed by confocal microscopy.

Confocal microscopy

For colocalization studies, cells were seeded overnight in Lab-Tek chambers (Nalgene Nunc, Rochester, NY) and cotransfected with the plasmids of interest or siRNA targeting CIMPR gene, by using TransPass HeLa transfection reagent. Confocal microscope images of cells 24 to 48 h after transfection were captured on a Zeiss LSM 510 confocal microscope or by using the 458-nm line of an Ar laser with a 465–505 emission filter for CFP, the 488-nm line of an Ar laser with a 505–550 emission filter (GFP), a 543-nm HeNe laser line with a 560–615 emission filter line for mCherry/mRFP. Images were captured with a Plan-Apochromat 1.4 NA 63×oil-immersion objective. Cells expressing both proteins were selected for z-sectioning. Z stacks were taken by using a pinhole of 0.5 Airy unit for both channels. Images were analyzed with ImageJ and Zeiss Image Examiner software and prepared by Adobe Photoshop 7.0.

Statistics

Results are presented as the mean ± SEM from three independent experiments. Two group comparisons were performed by using Student's *t* test. Multiple group comparisons were performed by using one-way analysis of variance and Fisher's least significant difference.

Results

ATRA reduces the number of nonacidified autophagosomes

To investigate the role of retinoic acid and analogues, we initially generated a stable HeLa cell line expressing LC3 fused to the carboxy terminus of CFP (HeLa-LC3). Attempts to generate EYFP-, GFP-, or mCherry-LC3 stable cell lines were unsuccessful, presumably because of the toxic effects of these fluorescent proteins when expressed over the long term as LC3 fusion proteins. The stable cell line is expressing CFP-LC3-I, which exhibits diffused cytosolic and nuclear distribution. Cleavage of a small carboxy-terminus portion from LC3-I and lipid conjugation generates LC3-II, a protein that has been shown specifically to associate with double membranes of maturating autophagosomes (AUTs) and decorates both the cytosolic and luminal sides of the organelle (2, 13, 18, 28), thus appearing as distinct punctuate structures. The ratio of LC3-I to LC3-II correlates very well with the total number of AUTs present at any time, and for that reason has been extensively used as measurement for steady-state levels of maturing AUTs. The ratio of LC3-I/LC3-II is not informative on the maturation level of AUTs or the degree of their acidification.

Treatment of HeLa-LC3 cells with 1 μM ATRA for 48 h resulted in substantial reduction of CFP-LC3-positive structures, whereas treatment with 0.5 μM of rapamycin (known activator of autophagy) induced a robust increase of CFP-LC3 structures (Fig. 1Aa). To confirm that this observation is not limited to the stable cell line, we treated CFP-LC3 transiently transfected HeLa cells and obtain similar results (Fig. 1Ac). In both cases, ATRA reduced CFP-LC3 structures by almost 50% (Fig. 1B) but did not affect the ratio of CFP-LC3-I to CFP-LC3-II (Fig. 1C). Rapamycin treatment though resulted in a substantial reduction of the CFP-LC3-I to CFP-LC3-II ratio. Surprisingly, ATRA treatment did not affect the abundance of mCherry-LC3 positive AUTs in transiently transfected HeLa cells (Fig. 1Ab). Given that CFP is very susceptible to quenching under acidic conditions, whereas mCherry is not, our data suggested that ATRA either increases acidification of autophagosomes (amphisomes) or increase the autophagosome–lysosome fusion rate.

ATRA does not affect the levels of upstream regulators of autophagy

Induction of AUT biogenesis requires two complexes. The first one, that initiates vesicle formation, contains the class III PI3K (Vps34), Beclin-1/Atg6, Atg14, and Vps15/p150 and is

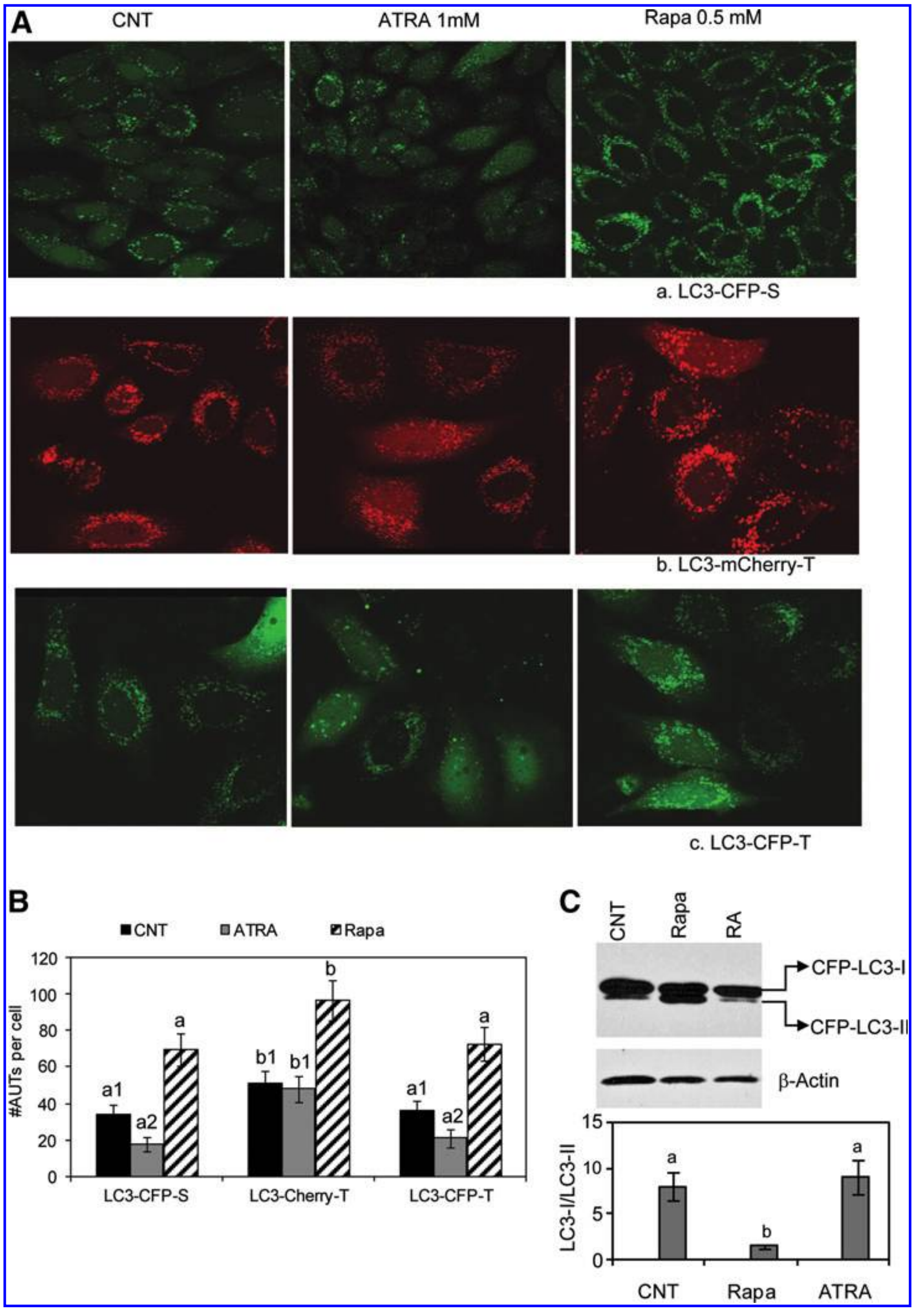

FIG. 1. All-*trans*-retinoic acid (ATRA) reduces the number of nonacidified AUTs. (A) Effect of ATRA and rapamycin (Rapa) on abundance of AUTs. **(a)** CFP-LC3 stably transfected HeLa cells were treated with ATRA or Rapa for 48 h. **(b)** mCherry-LC3 transiently transfected HeLa cells were treated with ATRA or Rapa for 48 h. **(c)** CFP-LC3 transiently transfected HeLa cells were treated with ATRA or Rapa for 48 h. For these experiments, cells were plated in Lab-Tek chambers the day before transfections or treatments. At the end of the experiments, cells were processed for confocal microscopy. **(B)** Quantification of the number of AUTs per cell in CFP-LC3-S (stable cell line), Cherry-LC3-T (transiently transfected), and CFP-LC3-T (transiently transfected) transfected cells treated with ATRA or untreated. For quantification, cells were optically sliced on a confocal microscope (see Materials and Methods) and then maximal-intensity z-projections were generated for each cell to visualize all AUTs. LSM images were exported as TIFF files, and the number of AUTs was quantified by using Image J. The data are presented as the average number of AUTs in each group. Treatments with different superscripts are statistically different. (b > a, b > a1, a > a1 > a2, b1 > a1). Data shown are the mean ± SEM from three independent experiments. **(C)** Parallel cultures of CFP-LC3-S cells were collected after 48 h of treatment, and total cell lysates were separated with SDS-PAGE and subjected to immunoblotting with anti-LC3 and anti-β-actin. The results are representative of three independent experiments. The intensity of the bands was quantified by Image J, and the ratio of LC3-I to LC3-II was calculated. Bars represent the mean ± SEM from three independent experiments. (To see this illustration in color the reader is referred to the web version of this article at www.liebertonline.com/ars).

highly controlled by Beclin-1. Beclin-1, the mammalian homologue of ATG6, was the first protein shown to be indispensible for autophagy in mammals (3, 23, 26). The second complex, responsible for the vesicle nucleation, contains Atg1/ULK1, mAtg13, mAtg13-associated proteins FIP200, and Atg101 in mammalian cells, the association of which is controlled by mTOR (30). Autophagy is negatively regulated by the serine/threonine kinase mTOR (mammalian target of rapamycin) (29, 48). Phosphorylated mTOR (pmTOR) is part of the induction complex and acts as a negative regulator of autophagy (43). In addition, activated mTOR induces hyperphosphorylation of Atg13, which reduces its binding affinity to other Atg interacting proteins, thereby inhibiting autophagy (19). One well-characterized pathway for mTOR activation involves Akt1 activation. Akt1 phosphorylates and inhibits the tuberous sclerosis complex 2 (TSC2) (39). TSC2 negatively regulates mTOR by acting as a GTPase-activating protein (GAP) for the small GTPase Rheb, which binds and activates mTOR (27). Therefore, elevated levels of phosphorylated Akt1 (pAkt1) promote conditions that inhibit autophagy.

To investigate whether ATRA affects the levels of AUTs by inhibiting induction of autophagosome formation, we examined the levels of Beclin-1, pmTOR, and pAkt1 in HeLa cells treated for 12, 24, and 48 h. Our results indicate that ATRA did not affect the total levels of Beclin-1, Akt1, Akt2, Akt3, and mTOR, and neither the levels of pmTOR and pAkt1 (Fig. 2). These data suggest that ATRA does not inhibit induction of AUT formation.

The effect of ATRA on AUT maturation is not mediated by the RARα/β/γ and RXR receptors

To investigate whether the effect of ATRA on AUT maturation is mediated by the classic retinoid acid receptors, we perform studies in the presence of receptor-specific antagonists and agonists. Two distinct classes of nuclear retinoid receptors are termed RARs and RXRs, each of which has three distinct subtypes, α, β, and γ. The RARs bind ATRA and 9-*cis*-RA with high affinity, whereas the RXRs bind 9-*cis*-RA selectively (4). At high doses, though (>10 μM), ATRA can slightly transactivate RXRs.

Treatment of CFP-LC3 stably transfected HeLa cells with CD2665 (10 μM) did not block the effect of ATRA (1 μM) in reducing the number of CFP-LC3 structure (Fig. 3), and treatment with CD2665 alone had no effect. CD2665 is a selective RARα/β/γ antagonist, with KD values of 0.1, 0.3, and 1 μM for RARγ, RARβ, and RARα, respectively (24). Actually, the effect of ATRA in reducing the number of CFP-LC3-positive structures was even more pronounced in the presence of CD2665. Binding of CD2665 to RARs could increase the bioavailability and binding of ATRA to another target. Although the effect of ATRA is not expected to be mediated by the RXRs, we subjected CFP-LC3 HeLa cells to treatment with DCHA, a highly potent and specific agonist of RXRs, and did not observe any significant effect. These results strongly suggest that the effect of ATRA is not mediated by the classic RARs and RXRs receptors.

ATRA changes the fluorescent properties of the mCherry-GFP-LC3 pH-sensitive reporter

CFP-, EYFP- and GFP-LC3 are being widely used as markers of maturing AUTs. However, these fluorescent proteins are acid labile with a pK_a of 6.0 (45), making it impossible to monitor AUTs after they become acidified (amphisomes) or fused with lysosomes. The luminal pH of late endosomes have a pH of about 5.5, and lysosomes have a pH of about 4.7 (50).

Fusion of the monomeric red fluorescent protein mCherry to LC3 alleviates some of these problems. The pK_a of mCherry

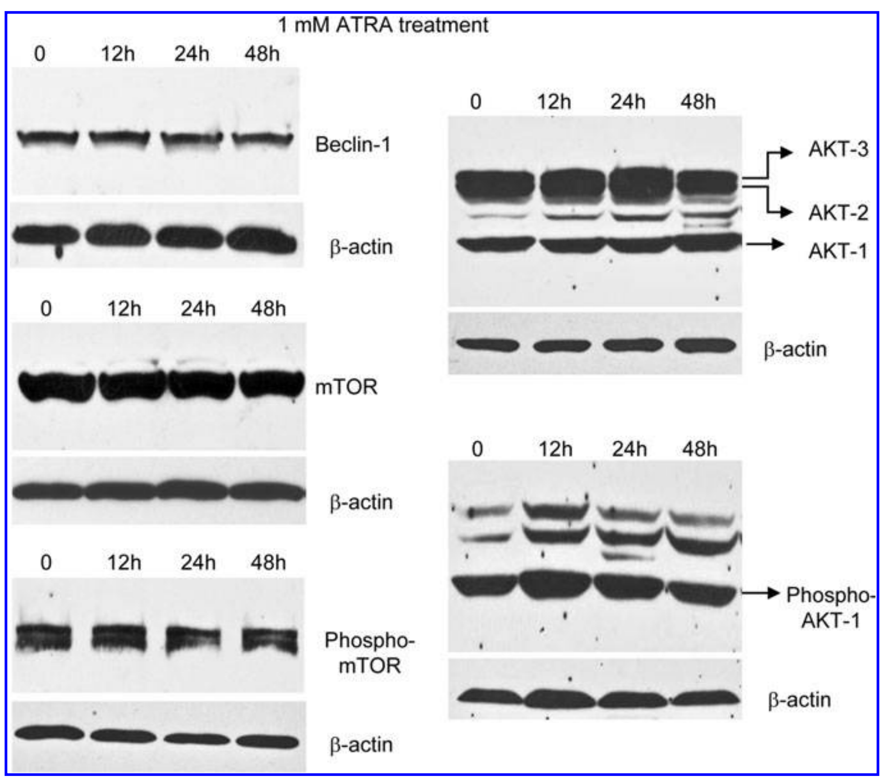

FIG. 2. ATRA treatment in HeLa cells does not affect expression of critical regulators of autophagy. HeLa cells were treated with ATRA for the indicated time points. At the end of the incubation period, total cell lysates were prepared, and equal amounts of proteins were separated on SDS-PAGE. Levels of Beclin-1, mTOR, phospho-mTOR, pan (Total) Akt, and phospho-Akt1 were evaluated with immunoblotting. Phosphorylated-mTOR levels were assessed by using a phospho-mTOR antibody specific for phosphorylation on Ser^{2448}, and phosphorylated-Akt1 levels were assessed by using a phospho-Akt1 antibody specific for phosphorylation on Ser^{473}. β-actin was used as a protein-loading control.

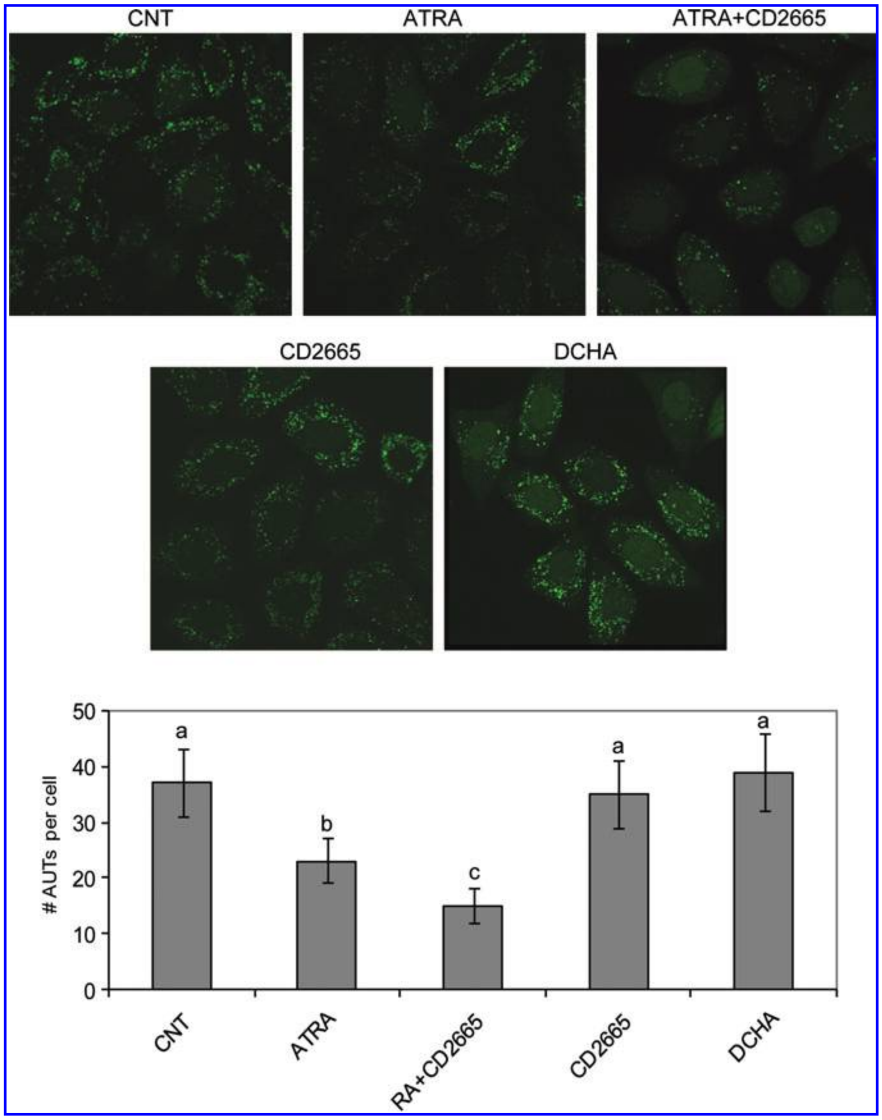

FIG. 3. The effect of ATRA on AUT maturation is not mediated by the RARα/β/η and RXR receptors. CFP-LC3 stably transfected cells were cultured on chamber slides and treated with 1 μM ATRA, 10 μM CD2665, 10 μM DCHA, or 1 μM ATRA + 10 μM CD2665 in combination. The number of AUTs per cell in each group was measured as described earlier. Data shown are the mean ± SEM from three independent experiments. (To see this illustration in color the reader is referred to the web version of this article at www.liebertonline.com/ars).

is < 4.5, making the protein very acid stable. As we showed earlier in this study, the number of mCherry-LC3–positive AUTs is much higher than that of CFP-LC3–positive AUTs. Simultaneously to detect both nonacidified and acidified AUTs, a mCherry-GFP double-tagged LC3 strategy recently was devised (38). Expression of mCherry-GFP-LC3 results in yellow-punctuated structures, which are nonacidified AUTs, and red structures, which are either amphisomes or autophagolysosomes. In the present study, treatment of mCherry-GFP-LC3–transfected HeLa cells resulted in substantial shift of the number of yellow-punctuated AUTs in favor of red-labeled AUTs (Fig. 4). After 48 h of ATRA treatment, almost half of the AUTs displayed red fluorescence only, thus confirming our earlier hypothesis that ATRA promotes acidification of maturing AUTs or increases the rate of autophagosome-lysosome fusion.

ATRA induces translocation of CIMPR to acidified AUTs

As we showed, the effect of ATRA in promoting acidification of AUTs is not mediated by the classic RAR and RXR receptors. Earlier studies identified CIMPR as a target for retinoic acid, and showed that retinoic acid can induce translocation of the receptor from perinuclear compartments to uncharacterized vesicular structures. The best-described function of CIMPR is to transport mannose-6-phosphate (M6P)-bearing glycoproteins from TGN to endosomal/prelysosomal compartments. The CIMPR is one of two transmembrane proteins that bind M6P tags on acid hydrolase precursors in the TGN that are destined for transport to the lysosome. The other protein is the cation-dependent mannose-6-phosphate receptor (CDMPR). Newly synthesized lysosomal enzymes are posttranslationally modified to contain M6P residues on their N-linked oligosaccharides. The M6P residues enable enzymes to bind to CIMPR (and CDMPR) receptors in the TGN. The ligands bind in one of the repeats of the large luminal domain. The receptor/ligand complexes cluster into clathrin-coated transport vesicles and travel to acidic prelysosomal compartments where the low pH causes dissociation of the receptor–ligand complex. The free M6P receptors can travel to the plasma membrane or back to the TGN to reinitiate another cycle of biosynthetic enzyme transport.

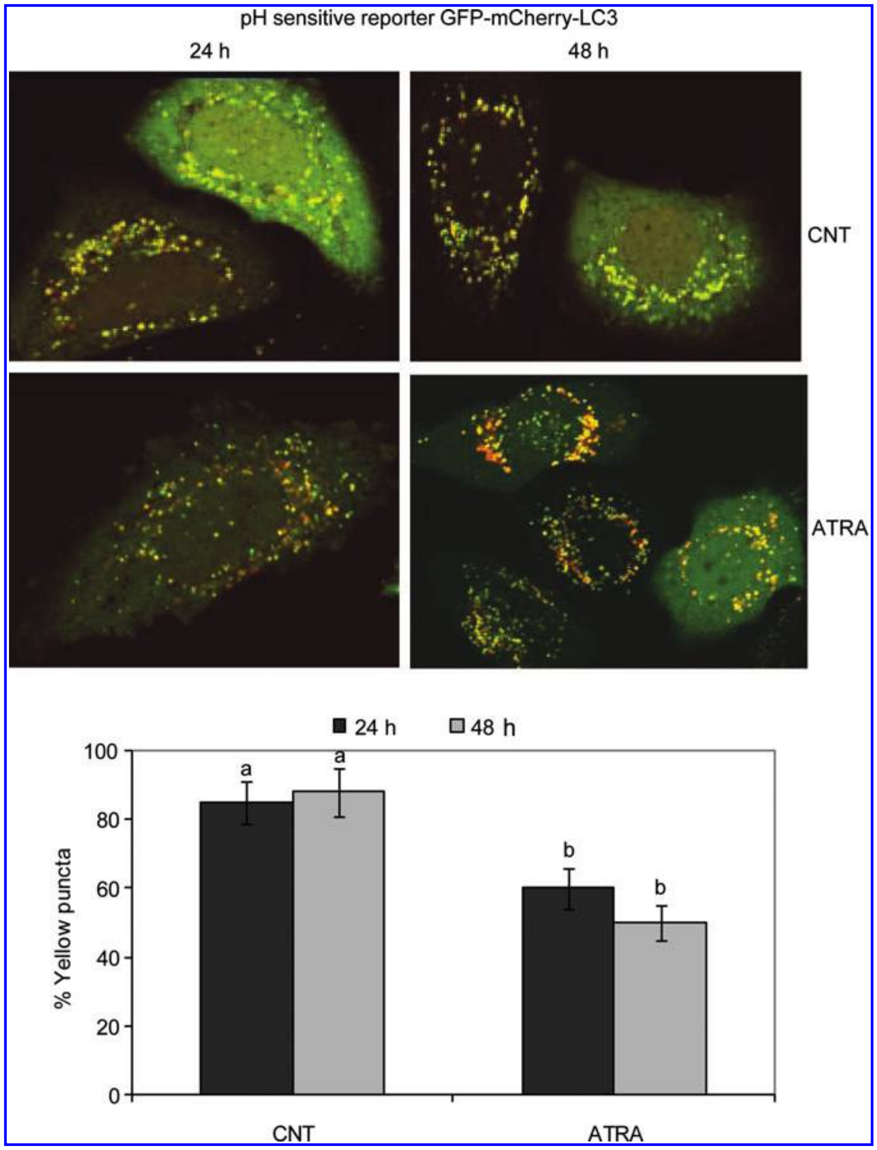

FIG. 4. ATRA treatment induces acidification of AUTs, as evaluated by using the pH-sensitive reporter GFP-mCherry-LC3. HeLa cells were transfected with GFP-LC3-mCherry, and either left untreated or treated with 1 μM ATRA for 24 and 48 h, respectively. After the indicated period of treatments, cells were prepared for live imaging by using confocal microscopy. The number of yellow and red punctuate structures was determined as described earlier. The data are presented as percentage of yellow puncta in control cells or cells treated with ATRA for the indicated time points. Data shown are the mean $\pm$ SEM from three independent experiments. (To see this illustration in color the reader is referred to the web version of this article at www.liebertonline.com/ars).

To determine whether RA induces translocation of the CIMPR in maturing autophagosomes, we prepared mGFP- and mRFP-tagged CIMPR constructs. The fluorescent tag was inserted in the carboxy terminus of CIMPR, which is the cytoplasmic domain of the protein, to ensure that acidified organelles will not quench the fluorescent signal. We initially transfected the CFP-LC3 stable HeLa cell line with CIMPR-mRFP and examined whether it colocalizes with AUTs in ATRA-treated (Fig. 5Ab) or -untreated cells (Fig. 5Aa). CIMPR-mRFP was localized mostly in perinuclear compartments (presumably TGN), some vesicular compartments, and plasma membrane. Treatment with ATRA induced a significant redistribution of CIMPR-mRFP to peripheral vesicular compartments, but those were not CFP-LC3–labeled AUTs (Fig. 5Ab). We also co-transfected ATRA-treated and -untreated HeLa cells with mCherry-LC3 and CIMPR-GFP. Even in the absence of ATRA, we noticed some co-localization of CIMPR-GFP with mCherry-LC3–labeled AUTs (Fig. 5Ba). In ATRA-treated cells, significant translocation of CIMPR-GFP in mCherry-LC3–labeled AUTs was noticed (Fig. 5Bb). These data show that retinoic acid induces redistribution of CIMPR in acidified AUTs or autophagolysosomes.

In the previous experiments, we showed that ATRA induces the translocation of CIMPR in an acidic compartment that is also positive for LC3. This compartment can be either an amphisome or an autophagolysosome. Autophagolysosomes are also positive for LAMP-1, a lysosomal marker protein. Transfection of ATRA-treated HeLa cells with CIMPR-GFP and LAMP-1-RFP and confocal microscopy indicated that CIMPR is not recruited in LAMP-1–positive structures (Fig. 6). This result suggests that retinoic acid induces redistribution of CIMPR in amphisomes (acidified AUTs) and not in autophagolysosomes.

siRNA-mediated knockdown of endogenous CIMPR induces large accumulation of nonacidified AUTs and Rab9-positive endosomes, but has no effect on abundance of lysosomes

Our studies suggest that CIMPR may play a critical role in mediating the effects of retinoic acid on AUT maturation. We

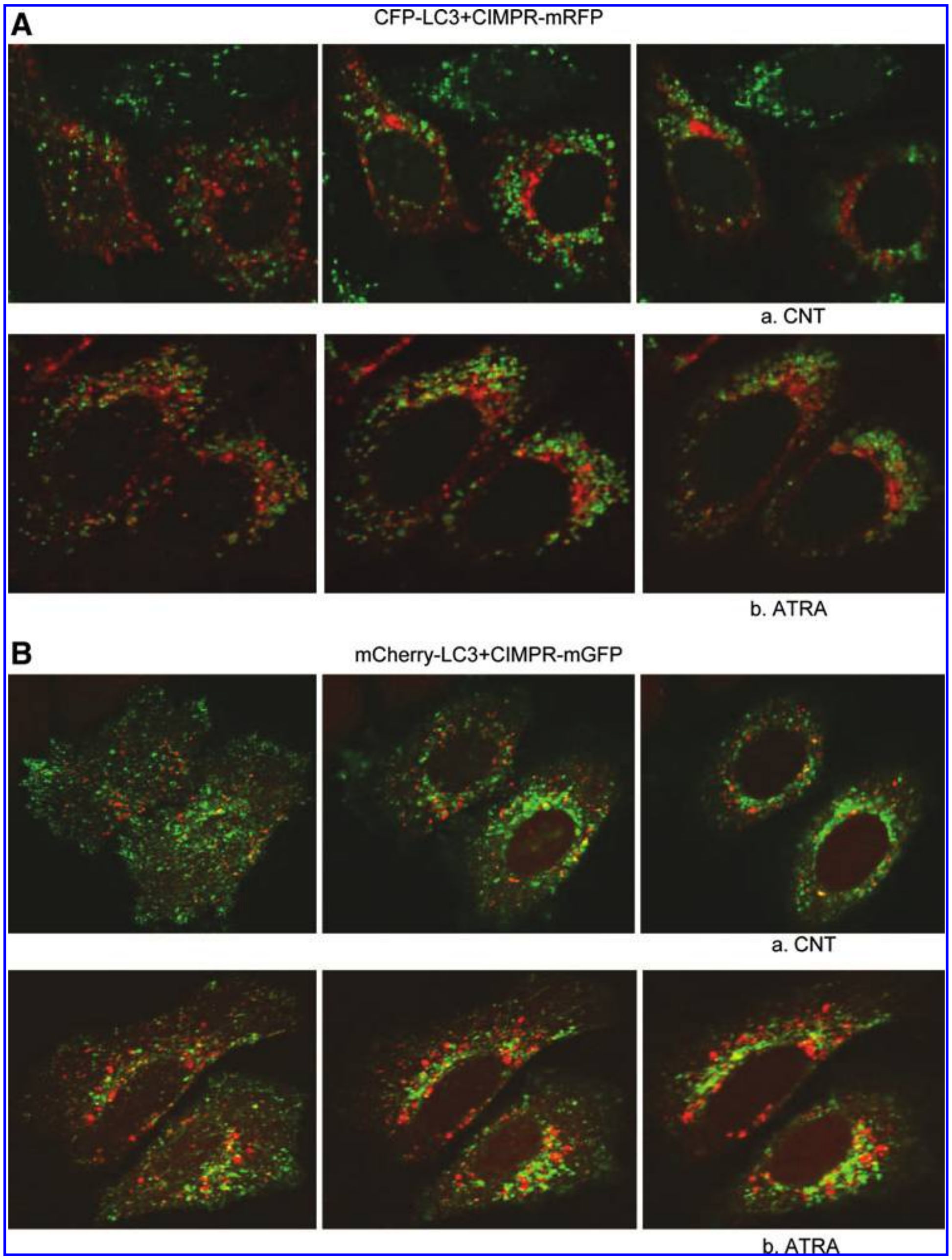

FIG. 5. ATRA treatment induces redistribution of CIMPR from TGN to acidified LC3-positive structures. (A) CFP-LC3 stably transfected HeLa cells, treated with ATRA or untreated, were transfected with CIMPR-mRFP; 48 h after transfection, live cell imaging was performed with confocal microscopy. **(B)** HeLa cells, either treated with ATRA or left untreated, were co-transfected with mCherry-LC3 and CIMPR-mGFP and subjected to confocal microscopy. The images are Z-sections and obtained as described earlier. (To see this illustration in color the reader is referred to the web version of this article at www.liebertonline.com/ars).

next asked whether downregulation of the endogenous levels of CIMPR could affect autophagy. We used a company-validated siRNA against CIMPR in the CFP-LC3 stable cell line and were able to document a dose-dependent downregulation of endogenous CIMPR protein levels (Fig. 7A). Transfection of CFP-LC3 cells with 10 n*M* (final concentration) siRNA resulted in a remarkable decrease in the ratio of CFP-LC3-I to CFP-LC3-II (Fig. 7B) and a large accumulation of LC3-CFP–positive structures. The siRNA-CIMPR–mediated increase of AUTs could not be reversed by ATRA, further suggesting that the effect of retinoic acids on AUTs is mediated primarily by CIMPR. Immunocytochemistry for endogenous CIMPR in siRNA-transfected CFP-LC3 cells indicated that complete silencing was observed in more than 80% of the cells. Remarkably, the few cells found in which silencing of CIMPR was not effective had normal levels of AUTs (Fig. 7C). Transfection of HeLa cells with siRNA against CIMPR and the pH-sensitive reporter mCherry-GFP-LC3 indicated that accumulated AUTs were nonacidified AUTs (yellow punctuates) (Fig. 7D). Treatment with ATRA resulted in a slightly decreased ratio of yellow-to-red punctuates, presumably because of incomplete CIMPR silencing in a portion of cells. This last piece of data suggests that CIMPR may be involved in AUT acidification, and that maturation is a prerequisite for physiologic turnover of newly synthesized AUTs. To determine whether downregulation of CIMPR affects the abundance of endosomes or lysosomes or both, we co-transfected HeLa cells with siRNA against CIMPR and one of either cerulean-Rab5, cerulean-Rab7, cerulean-Rab9, or Lamp1-RFP. The cells transfected with Lamp1 were also stained with LysoSensor Green. We did not observe any effect on abundance of Rab5- and Rab7-positive endosomes (data not shown).

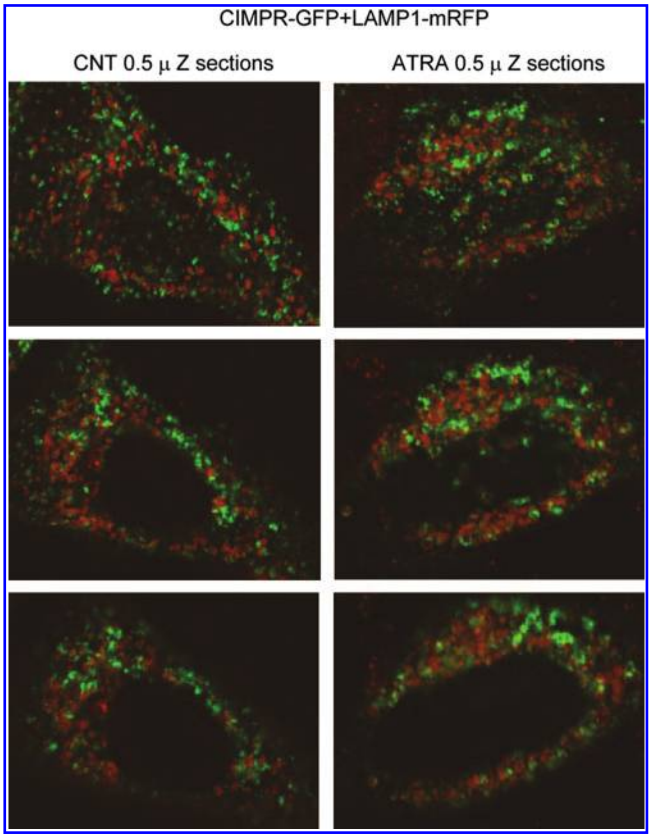

FIG. 6. ATRA does not redistribute CIMPR to LAMP1-positive organelles. HeLa cells were co-transfected with CIMPR-mGFP and LAMP1-mRFP and either treated with 1 μM ATRA or left untreated. At 48 h later, cells were analyzed by using confocal microscopy and Z-sectioning. (To see this illustration in color the reader is referred to the web version of this article at www.liebertonline.com/ars).

However, knockdown of CIMPR resulted in increased numbers of Rab9-positive endosomes (Fig. 8A). Knockdown of CIMPR also did not affect lysosome abundance, but reduced the number of Lamp1-positive structures that were also labeled with LysoSensor Green, indicating reduced lysosomal acidification (Fig. 8B). It should be noted that LysoSensor Green stains other acidified structures in addition to lysosomes, and that, in addition to CIMPR, the cation-dependent mannose-phosphate receptor (CDMPR) is also involved in acidification of late endosomes. The contribution of each receptor in different compartments is unknown. Our data clearly indicate that CIMPR is involved in acidification of AUTs and at least partially in the acidification of lysosomes. Accumulation of Rab9-positive structure in cells with reduced CIMPR may suggest that AUTs fuse with a subset of Rab9 endosomes, and may be dependent on this process for their acidification. However, Rab9-positive endosomes fuse also with lysosomes, and we have not observed significant colocalization of AUTs and Rab9-positive endosomes (28).

It could be that accumulation of Rab9-positive endosomes is due to their reduced fusion with lysosomes. Lysosomes do not carry CIMPR, and their acidification depends primarily on their fusion with late endosomes. However, we found that acidified AUTs carry their own CIMPR, and direct acidification of AUTs without fusion with endosomes cannot be excluded.

Discussion

Turnover of most long-lived proteins, macromolecules, biologic membranes, and whole organelles, including mitochondria, ribosomes, endoplasmic reticulum, and peroxisomes, is mediated by autophagy. A basal form of autophagy is essential for maintenance of cellular homeostasis, and an inducible form becomes activated under stress conditions (nutrient deprivation, infections, and toxins). The overall process of autophagy can be generally divided into three parts; induction of the autophagosomal membranes, functional and structural autophagosome maturation, and fusion with lysosomes. Our study suggests that retinoic acids are not involved in autophagosome biogenesis, but may play a crucial role in autophagosome acidification and maturation.

The initial formation of an autophagosomal membrane takes place by wrapping the degradative cargo within a double membrane, which eventually elongates to form a vesicle called an autophagosome. Autophagosomes then undergo a maturation process consisting of multiple fusion events with endosomal compartments (13). These fusion events are thought to be responsible for the enrichment of autophagosomes with the vacuolar-type proton ATPase that mediates acidification of AUTs to amphisomes. Therefore, one possible explanation for increased AUT acidification by ATRA is that ATRA increases the fusion rate of autophagosomes with endosomes. Alternatively, CIMPR may mediate the transportation of the proton ATPase to autophagosomes directly from the Golgi network. Our data showing accumulation of nonacidified AUTs after silencing of CIMPR strongly suggest the involvement of this receptor in AUT acidification.

CIMPR is constitutively expressed in all cells and cycles through a number of post-Golgi compartments, including the plasma membrane, early/sorting and recycling endosomes, but are predominantly found in late endosomes (3). In addition to binding lysosomal hydrolases, CIMPR can bind other mannose 6-phosphate–tagged proteins and also untagged proteins and can facilitate their clearance or activation or both. This includes a variety of growth factors, such as TGF-β precursor, proliferin and renin precursor, as well as endocytosis-mediated degradation of IGF-II. However, the main function of CIMPR is to deliver hydrolases to lysosomes and other vesicular structures (14). At the TGN, the CIMPR captures newly synthesized lysosomal enzymes through their mannose 6-phosphate–recognition signals. The ligand–receptor complexes are then transported to endosomes by vesicular transport, which is characterized by one of the clathrin-adaptor complexes, adaptor protein-1 (AP-1), and a recently identified family of monomeric clathrin-adaptor proteins, the GGAs (Golgi-localized, γ-ear-containing, adenosine diphosphate-ribosylation factor–binding proteins). After fusion with endosomes and the release of its ligands into the compartments, the receptor then recycles back to the TGN for a second round of transport.

Based on electron microscopy, subcellular fractionation studies, and immunofluorescence studies, localization of endogenous CIMPR in a subset of autophagosomes was previously reported (11, 17). In agreement with these studies, we found fluorescently tagged CIMPR to acidified AUTs in increasing amounts under ATRA treatment, which suggest

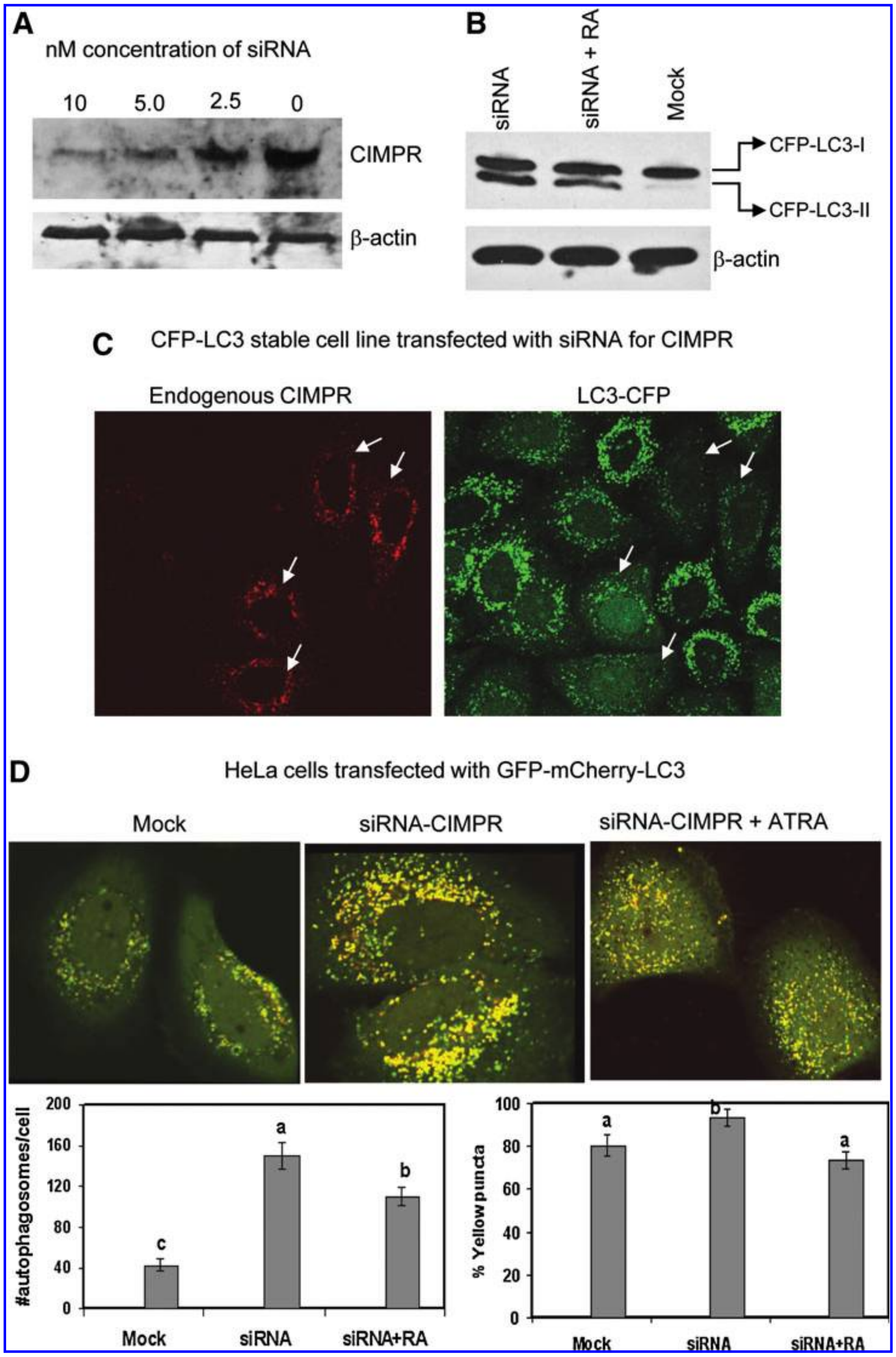

FIG. 7. siRNA-mediated knockdown of CIMPR induces accumulation of nonacidified AUTs that cannot be reversed by treatment with ATRA. (A) HeLa cells were cultured on six-well plates and transfected with increasing concentrations (0, 2.5, 5.0, and 10 n*M*) siRNA against CIMPR. Cells were lysed 48 h after transfection, and equal amounts of whole-cell lysates were separated with SDS-PAGE. CIMPR levels were measured with immunoblotting by using a monoclonal anti-CIMPR antibody (clone MEM-238). β-Actin immunostaining served as a protein-loading control. **(B)** CFP-LC3, stably transfected, grown on six-well plates, were transfected either with 10 n*M* siRNA against CIMPR or mock transfected by using a scrambled siRNA and treated with 1 μM ATRA or left untreated. 48 h after transfection. Total cell lysates were obtained and subjected to Western blot analysis by using an anti-LC3 antibody. **(C)** CFP-LC3 cells grown on chambered coverslips were transfected with 10 n*M* siRNA against CIMPR. At 48 h after transfection; the cells were fixed and processed for immunofluorescence staining by using an anti-CIMPR monoclonal antibody (clone 2G-11) and Alexa Fluor-555 goat anti-mouse fluorescent secondary antibody, and examined with confocal microscopy. **(D)** HeLa cells grown on chambers were treated with ATRA or left untreated and co-transfected with GFP-mCherry-LC3 and siRNA against CIMPR. The number of yellow and red punctate structures was estimated by using confocal microscopy, as described previously. The total number of AUTs and the percentage of yellow puncta in each treatment group were analyzed separately. Treatments with different superscripts are statistically different. Data shown are the mean ± SEM from three independent experiments. (To see this illustration in color the reader is referred to the web version of this article at www.liebertonline.com/ars).

that CIMPR also may be involved in delivering acid hydrolases to these structures, creating degradative autophagosomes. Knockdown of endogenous CIMPR leads to substantial accumulation of nonacidified AUTs, which further suggests that acidification and possible acquisition of hydrolases may be an important event in the maturation of all AUTs and not only amphisomes, and it may be a requirement for fusion with lysosomes.

A number of experimental and epidemiologic studies have suggested that loss of retinoid acid responsiveness is linked to carcinogenesis. Furthermore, several natural and synthetic retinoids have been shown to be highly effective in inhibiting chemically induced carcinogenesis in experimental animals by regulating cell proliferation and differentiation (31). Perturbations in the autophagic process and mutations in CIMPR also have been linked to several types of tumors (7, 40). Our

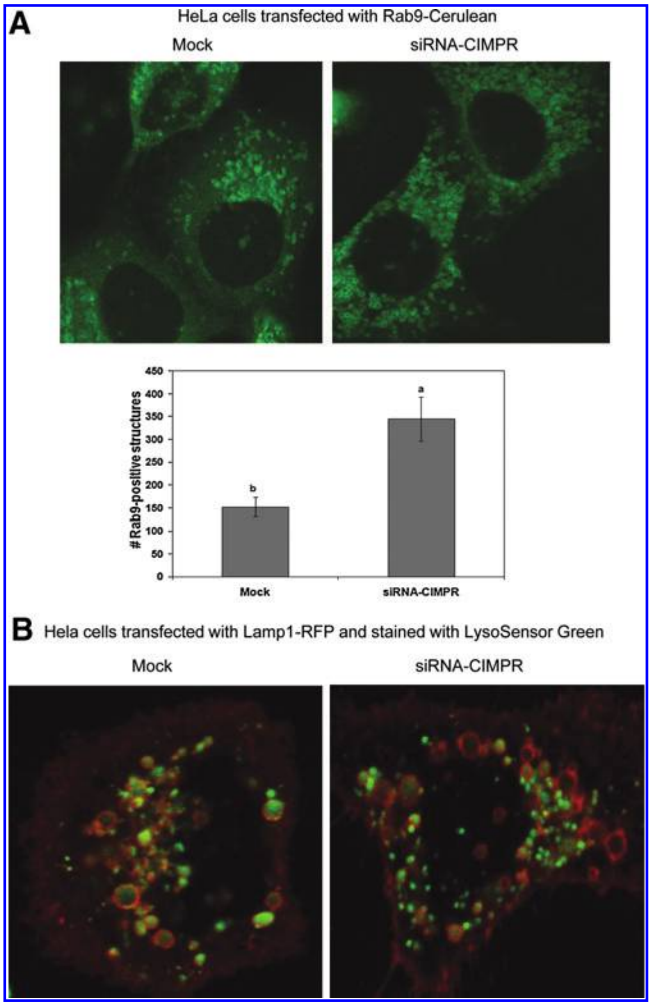

FIG. 8. siRNA-mediated knockdown of CIMPR induces accumulation of Rab9-positive endosomes and reduces lysosome acidification. (A) HeLa cells grown on chambers were co-transfected with Rab9-Cerulean and siRNA against CIMPR or a scrambled siRNA. At 48 h after transfection, the number of Rab9-positive structures was estimated by using the method described earlier. **(B)** HeLa cells were co-transfected with Lamp1-RFP and siRNA against CIMPR or a scrambled siRNA. At 48 h after transfection, the cells were incubated for 1 h with 2 μM LysoSensor Green, washed several times with warm medium, and visualized with confocal microscopy. (To see this illustration in color the reader is referred to the web version of this article at www.liebertonline.com/ars).

data suggest that retinoic acid positively affects autophagy by promoting maturation of AUTs. It is therefore tempting to speculate that part of the retinoid antitumor effects may be mediated through the process of autophagy.

Acknowledgments

This work was supported by the Virginia-Maryland Regional College of Veterinary Medicine and the Maryland Agricultural Experiment Station.

Author Disclosure Statement

No competing financial interests exist.

References

1. Ahuja HS, James W, and Zakeri Z. Rescue of the limb deformity in hammertoe mutant mice by retinoic acid-induced cell death. *Dev Dyn* 208: 466–481, 1997.
2. Bampton ETW, Goemans CG, Niranjan D, Mizushima N, and Tolkovsky AM. The dynamics of autophagy visualized in live cells. *Autophagy* 1: 23–36, 2005.
3. Bonifacino JS and Rojas R. Retrograde transport from endosomes to the trans-Golgi network. *Nat Rev Mol Cell Biol* 7: 568–579, 2006.
4. Chambon P. A decade of molecular biology of retinoic acid receptors. *FASEB J* 10: 940–954, 1996.
5. Cheng J, Ohsaki Y, Tauchi-Sato K, Fujita A, and Fujimoto T. Cholesterol depletion induces autophagy. *Biochem Biophys Res Commun* 351: 246–252, 2006.
6. Cuervo AM. Autophagy: many paths to the same end, *Mol Cell Biochem* 263: 55–72, 2004.
7. De Souza AT, Hankins GR, Washington MK, Orton TC, and Jirtle RL. M6P/IGF2R gene is mutated in human hepatocellular carcinomas with loss of heterozygosity. *Nat Genet* 11: 447–449, 2004.
8. Delia D, Aiello A, Lombardi L, Pelicci PG, Grignani F, Grignani F, Formelli F, Menard S, Costa A, Veronesi U, and Pierotti MA. *N*-(4-hydroxyphenyl) retinamide induces apoptosis of malignant hemopoietic cell lines including those unresponsive to retinoic acid. *Cancer Res* 53: 6036–6041, 1993.
9. Dennis PA and Rifkin DB. Cellular activation of latent transforming growth factor beta requires binding to the cation-independent mannose 6-phosphate/insulin-like growth factor type II receptor. *Proc Natl Acad Sci U S A* 88: 580–584, 1991.
10. Duester G. Retinoic acid synthesis and signaling during early organogenesis. *Cell* 134: 921–931, 2008.
11. Dunn WA Jr. Studies on the mechanisms of autophagy: maturation of the autophagic vacuole. *J Cell Biol* 110: 1935–1945, 1990.
12. Ebato C, Uchida T, Arakawa M, Komatsu M, Ueno T, Komiya K, Azuma K, Hirose T, Tanaka K, Kominami E, Kawamori R, Fujitani Y, and Watada H. Autophagy is important in islet homeostasis and compensatory increase of beta cell mass in response to high-fat diet. *Cell Metab* 8: 325–332, 2008.
13. Eskelinen L. Maturation of autophagic vacuoles in mammalian cells. *Autophagy* 1: 1–10, 2005.
14. Hawkes C and Kar S. The insulin-like growth factor-II/mannose-6-phosphate receptor: structure, distribution and function in the central nervous system. *Brain Res Brain Res Rev* 44: 117–140, 2004.
15. Høyer-Hansen M, Bastholm L, Mathiasen IS, Elling F, and Jäättelä M. Vitamin D analog EB1089 triggers dramatic lysosomal changes and Beclin 1-mediated autophagic cell death. *Cell Death Differ* 12: 1297–1309, 2005.
16. Itoh Y, Kawamata Y, Harada M, Kobayashi M, Fujii R, Fukusumi S, Ogi K, Hosoya M, Tanaka Y, Uejima H, Tanaka H, Maruyama M, Satoh R, Okubo S, Kizawa H, Komatsu H, Matsumura F, Noguchi Y, Shinohara T, Hinuma S, Fujisawa Y, and Fujino M. Free fatty acids regulate insulin secretion from pancreatic beta cells through GPR40. *Nature* 422: 173–176, 2003.
17. Jahreiss L, Menzies FM, and Rubinsztein DC. The itinerary of autophagosomes: from peripheral formation to kiss-and-run fusion with lysosomes. *Traffic* 9: 574–587, 2008.
18. Kabeya Y, Mizushima N, Ueno T, Yamamoto A, Kirisako T, Noda T, Kominami E, Ohsumi Y, and Yoshimori T. LC3, a

mammalian homologue of yeast Apg8p, is localized in autophagosome membranes after processing. *EMBO J* 19: 5720–5728, 2000.
19. Kamada Y, Funakoshi T, Shintani T, Nagano K, Ohsumi M and Ohsumi Y. Tor-mediated induction of autophagy via an Apg1 protein kinase complex, *J Cell Biol* 150: 1507–1513, 2000.
20. Kanazawa T, Taneike I, Akaishi R, Yoshizawa F, Furuya N, Fujimura S, and Kadowaki M. Amino acids and insulin control autophagic proteolysis through different signaling pathways in relation to mTOR in isolated rat hepatocytes. *J Biol Chem* 279: 8452–8459, 2004.
21. Kang JX, Li Y, and Leaf A. Mannose-6-phosphate/insulin-like growth factor-II receptor is a receptor for retinoic acid. *Proc Natl Acad Sci U S A* 94: 13671–13676, 1997.
22. Kassi E and Papavassiliou AG. Could glucose be a proaging factor? *J Cell Mol Med* 12: 1194–1198, 2008.
23. Kihara A, Kabeya Y, Ohsumi Y, and Yoshimori T. Beclin-phosphatidylinositol 3-kinase complex functions at the trans-Golgi network. *EMBO Rep* 2: 330–335, 2001.
24. Kim MJ, Ciletti N, Michel S, Reichert U, and Rosenfield RL. The role of specific retinoid receptors in sebocyte growth and differentiation in culture. *J Invest Dermatol* 114: 349–353, 2000.
25. Kornfeld S. Structure and function of the mannose 6-phosphate/insulinlike growth factor II receptors. *Annu Rev Biochem* 61: 307–330, 1992.
26. Liang XH, Jackson S, Seaman M, Brown K, Kempkes B, Hibshoosh H, and Levine B. Induction of autophagy and inhibition of tumorigenesis by Beclin 1. *Nature* 402: 672–676, 1999.
27. Long X, Lin Y, Ortiz-Vega S, Yonezawa K, and Avruch J. Rheb binds and regulates the mTOR kinase. *Curr Biol* 15: 702–713, 2005.
28. Mavrakis M, Lippincott-Schwartz J, Stratakis CA, and Bossis I. Depletion of type IA regulatory subunit (RIalpha) of protein kinase A (PKA) in mammalian cells and tissues activates mTOR and causes autophagic deficiency. *Hum Mol Genet* 15: 2962–2971, 2006.
29. Mavrakis M, Lippincott-Schwartz J, Stratakis CA, and Bossis I. mTOR kinase and the regulatory subunit of protein kinase A (PRKAR1A) spatially and functionally interact during autophagosome maturation. *Autophagy* 3: 151–153, 2007.
30. Mizushima N. The role of the Atg1/ULK1 complex in autophagy regulation. *Curr Opin Cell Biol* 22: 132–139, 2010.
31. Moon RC, Metha RG, and Rao, KVN. Retinoids and cancer in experimental animals. In: *The Retinoids: Biology, Chemistry, and Medicine,* 2nd ed. Edited by Sporn MB, Roberts AB, and Goodman DS. New York: Raven Press, 1994, pp. 573–595.
32. Mordier S, Deval C, Béchet D, Tassa A, and Ferrara M. Leucine limitation induces autophagy and activation of lysosome-dependent proteolysis in C2C12 myotubes through a mammalian target of rapamycin-independent signaling pathway. *J Biol Chem* 275: 29900–29906, 2000.
33. Morgan DO, Edman JC, Standring DN, Fried VA, Smith MC, Roth RA, and Rutter WJ. Insulin-like growth factor II receptor as a multifunctional binding protein. *Nature* 329: 301–307, 1987.
34. Nykjaer A, Christensen EI, Vorum H, Hager H, Petersen CM, Røigaard H, Min HY, Vilhardt F, Møller LB, Kornfeld S, and Gliemann J. Mannose 6-phosphate/insulin-like growth factor-II receptor targets the urokinase receptor to lysosomes via a novel binding interaction. *J Cell Biol* 141: 815–828, 1998.
35. O'Connell MJ, Chua R, Hoyos B, Buck J, Chen Y, Derguini F, and Hämmerling U. Retro-retinoids in regulated cell growth and death. *J Exp Med* 184: 549–555, 1996.
36. Ohtani S, Iwamaru A, Deng W, Ueda K, Wu G, Jayachandran G, Kondo S, Atkinson EN, Minna JD, Roth JA, and Ji L. Tumor suppressor 101F6 and ascorbate synergistically and selectively inhibit non-small cell lung cancer growth by caspase-independent apoptosis and autophagy. *Cancer Res* 67: 6293–6303, 2007.
37. Oshima A, Nolan CM, Kyle JW, Grubb JH, and Sly WS. The human cation-independent mannose 6-phosphate receptor: cloning and sequence of the full-length cDNA and expression of functional receptor in COS cells. *J Biol Chem* 263: 2553–2562, 1988.
38. Pankiv S, Clausen TH, Lamark T, Brech A, Bruun JA, Outzen H, Overvatin A, Bjorkoy G, and Johansen T. p62/SQSTM1 binds directly to Atg8/LC3 to facilitate degradation of ubiquitinated protein aggregates by autophagy. *J Biol Chem* 282: 24131–24145, 2007.
39. Potter CJ, Pedraza LG, and Xu T. Akt regulates growth by directly phosphorylating Tsc2. *Nat Cell Biol* 4:658–665, 2002.
40. Rajawat YS and Bossis I. Autophagy in aging and in neurodegenerative disorders. *Hormones (Athens)* 7: 46–61, 2008.
41. Rajawat YS, Hilioti Z, and Bossis I. Aging: central role for autophagy and the lysosomal degradative system. *Ageing Res Rev* 8: 199–213, 2009.
42. Rickmann M, Vaquero EC, Malagelada JR, and Molero X. Tocotrienols induce apoptosis and autophagy in rat pancreatic stellate cells through the mitochondrial death pathway. *Gastroenterology* 132: 2518–2532, 2007.
43. Schmelzle T and Hall MN. TOR, a central controller of cell growth. *Cell* 103: 253–262, 2000.
44. Schworer CM and Mortimore GE. Glucagon-induced autophagy and proteolysis in rat liver: mediation by selective deprivation of intracellular amino acids. *Proc Natl Acad Sci U S A* 76: 3169–3173, 1979.
45. Shaner NC, Steinbach PA, and Tsien RY. A guide to choosing fluorescent proteins. *Nat Methods* 2: 905–909, 2005.
46. Singh R, Kaushik S, Wang Y, Xiang Y, Novak I, Komatsu M, Tanaka K, Cuervo AM, and Czaja MJ. Autophagy regulates lipid metabolism. *Nature* 458: 1131–1135, 2009.
47. Teboul M, Guillaumond F, Gréchez-Cassiau A, and Delaunay F. The nuclear hormone receptor family round the clock. *Mol Endocrinol* 22: 2573–2582, 2008.
48. Wullschleger S, Loewith R, and Hall MN. TOR signaling in growth and metabolism. *Cell* 124: 471–484, 2006.
49. Yokoyama T, Miyazawa K, Naito M, Toyotake J, Tauchi T, Itoh M, Yuo A, Hayashi Y, Georgescu MM, Kondo Y, Kondo S, and Ohyashiki K. Vitamin K2 induces autophagy and apoptosis simultaneously in leukemia cells. *Autophagy* 4: 629–640, 2008.
50. Zen K, Biwersi J, Periasamy N, and Verkman AS. Second messengers regulate endosomal acidification in Swiss 3T3 fibroblasts. *J Cell Biol* 119: 99–110, 1992.

Address correspondence to:
Dr. Ioannis Bossis
Department of Veterinary Medicine
University of Maryland
8075 Greenmead Drive
College Park, MD 20742

E-mail: bossisi@umd.edu

Date of first submission to ARS Central, August 16, 2010; date of acceptance, September 2, 2010.

Abbreviations Used

AKT1 = RAC-α serine/threonine-protein kinase
ATRA = all *trans*-retinoic acid
CFP = cyan fluorescent protein
CIMPR = cation-independent mannose 6-phosphate receptor
DABCO = 1,4-diazabicyclo[2.2.2]octane
DMSO = dimethyl sulfoxide
FACS = fluorescence-activated cell sorting
HRP = horseradish peroxidase
IGFII = insulin-like growth factor 2
IGFIIR = insulin-like growth factor 2 receptor
LAMP1 = lysosomal-associated membrane protein 1
LC3 = light chain 3
M6P = mannose-6-phosphate
M6PR = mannose-6-phosphate receptor
mGFP = monomeric green fluorescent protein
mRFP = monomeric red fluorescent protein
mTOR = mammalian target of rapamycin
ORF = open reading frame
PI3K = phosphoinositide 3-kinase
RA = retinoic acid
RAR = retinoic acid receptor
RIPA = radioimmunoprecipitation
RXR = retinoid X receptor
SDS = sodium dodecylsulfate
SEM = standard error of the mean
siRNA = small interfering RNA
TGN = *trans*-Golgi network

This article has been cited by:

1. Dipak K. Das . 2011. Autophagy: A Story of Live or Let DieAutophagy: A Story of Live or Let Die. *Antioxidants & Redox Signaling* **14**:11, 2163-2164. [Citation] [Full Text] [PDF] [PDF Plus]